DETERMINISTIC CHAOS IN THE MICROSTRUCTURE OF RADIO PULSES OF PSR 0809+74

V. I. ZHURAVLEV AND M. V. POPOV
Institute for Space Research, Academy of Sciences

Abstract

480 single pulses from PSR 0809+74, recorded at 102.5 MHz with a time resolution of 10 μs, have been analyzed by the time delay technique in order to look for the parameters of deterministic chaos in the microstructure of radio pulses. The correlation dimension n was shown to be less than 5 in more than 20% of the analyzed pulses. This means that on such occasions the microstructure of pulsar radio emission with the time scales 10 to 100 μs may be determined by the behavior of a nonlinear dynamical system with comparatively small numbers of independent parameters. For example, the observed low dimensional chaos may result from a turbulence process associated with the outflow of plasma—as in versions of the polar cap model where microstructure can be interpreted as reflecting the spatial structure of relativistic plasma outflow in the radio emission region.

However, the correlation-time distribution demonstrates the tendency for microstructure to consist of a random sequence of unresolved micropulses in the majority of cases, which means in the framework of polar cap models the presence of well developed turbulence in the relativistic plasma outflow.

Introduction

Microstructure represents enormous variations in pulse intensity on time scales of the order of a few hundred microseconds. A useful way of quantifying the presence of microstructure is to compute the average autocorrelation function (ACF) of a number of individual pulses. By this technique microstructure time scales τ_μ have been measured for about a dozen pulsars (Cordes 1979; Kardashev *et al.* 1978). The general behavior of the microstructure ACF was shown to be well represented under the assumption that the received radiation is described by random Gaussian noise that has been amplitude modulated [the so-called amplitude modulated noise model (AMN)](Cordes 1976; Hankins and Boriakoff 1978; Cordes and Hankins 1979). The proposed model for the intensity of pulsar radio emission $S(t)$ is given by the product of a real amplitude modulation $a(t)$ and an uncorrelated stationary complex white noise process, $n(t)$ (Rickett 1975)

$$S(t) = a(t)n(t) \qquad (1)$$

A major implication of the AMN model is that micropulses do not provide a direct look at the coherent radio emission mechanism but represent a result of incoherent superposition by a large number of emitters. However, micropulse emission, being the shortest physically meaningful fluctuation of the radio emission, certainly reflects the physical condition in the region where they originated.

In our analysis we shall investigate the statistical properties of the amplitude-modulation function $a(t)$ using an approach and technique from the field of nonlinear dynamics. We shall attempt to determine whether a deterministic process underlies the microstructure intensity fluctuations in the case of pulsar radio emission.

Data analysis

We use the method of time delays (Ruelle 1981) to produce a representation of the dynamics from the single variable [microstructure intensity fluctuation $S(t)$] by reconstructing the trajectory of the system in phase space. The technique embeds the $S(t)$-curve in a space of dimension N. We can examine the nature of this trajectory and inquire whether the trajectory explores all available regions of phase space, or is confined to a subspace. If confined to a subspace, it may well lie on a fixed geometrical object, formally known as a manifold. It is often referred to as an attractor and in physical terms represents the asymptotic motion of the dynamics of the system. The presence of an attractor signifies a simplification of the dynamics of the system, since not all of the possible physical parameters are necessary to describe the system's behavior.

In our analysis we used the observations of single pulses of PSR 0809+74 at 102.5 MHz with a time resolution of 10 μs. N_s values of data $S(t)$ were binned into interval τ: $S(t_1), S(t_2), \ldots, S(t_N), t = t + (i-1)\tau$. Then for a given embedding dimension d we can construct the vectors

https://doi.org/10.1017/S0002731600155441 Published online by Cambridge University Press

$$S_i^d = \{S(t_i), S(t_i+\tau), S(t_i+2\tau), \ldots, \ldots, S(t_i+[d-1]\tau)\}, \quad (2)$$

where $i = (1,\ldots,N), N = N_s - (d-1)$. So, there are N vectors, which represent points in the d-dimensional space. To find the dimension of the object described by the trajectory, we utilize the method of Grassberger and Procaccia (1983a,b). From the vectors, constructed through the time delays, one can compute the correlation integral

$$C(r) = \frac{1}{N_s^2} \sum_{i,j=1}^{N} \theta(r - |S_i^d - S_j^d|), \quad (3)$$

where θ is the Heaviside function: $\theta(x) = 0$ for $x \leq 0$, and $\theta(x) = 1$ for $x > 0$. The function $C(r)$ counts the number of pairs of those points with a distance $|S_i^d - S_j^d|$ smaller than r. For sufficiently large embeding dimension d, small distances and large number of points N, Grassberger and Procaccia (1983b) showed that

$$C(r) \propto r^{\nu}, \quad (4)$$

where ν is referred to as the correlation dimension. This relation simply states that the number of points in a ball of radius ν scales with r. If the embedding dimension is smaller than the manifold's dimension then the points S_i occupy all of the available dimensions, giving $\nu \simeq n$. However, when the embedding dimension is sufficiently larger than the object is, then ν will be a lower limit to the Hausdorff–Besicovitch (or fractal) dimension of the object. In practice we determined ν for small r as

$$\nu = \lim_{r\sim 0} \frac{\log C(r)}{\log r}. \quad (5)$$

A second order entropy K_2 can be defined by the correlation integral $C(r)$

$$K_2 = \lim_{r\sim 0} \lim_{d\sim\infty} \frac{1}{\nu} \log \frac{C_d(r)}{C_{d+1}(r)} \leq K. \quad (6)$$

Entropy K_2 represents a lower limit to the metric or Kolmogorov entropy K_1, which is a measure for the internal information production of the system during its temporal evolution. The limiting cases $K_1 = 0$, and $K_1 \sim \infty$ characterize the situations of regular (*e.g.* periodic) and stochastic behavior of the system, respectively. If $K_1 > 0$, the system shows chaotic behavior. Since $K_2 \leq K_1, K_2 > 0$ is a sufficient condition for deterministic chaos. Furthermore, K_2 can be used to quantify the degree of chaos. It is related to the inverse predictability time (correlation time τ_{corr}) of the behavior of the system.

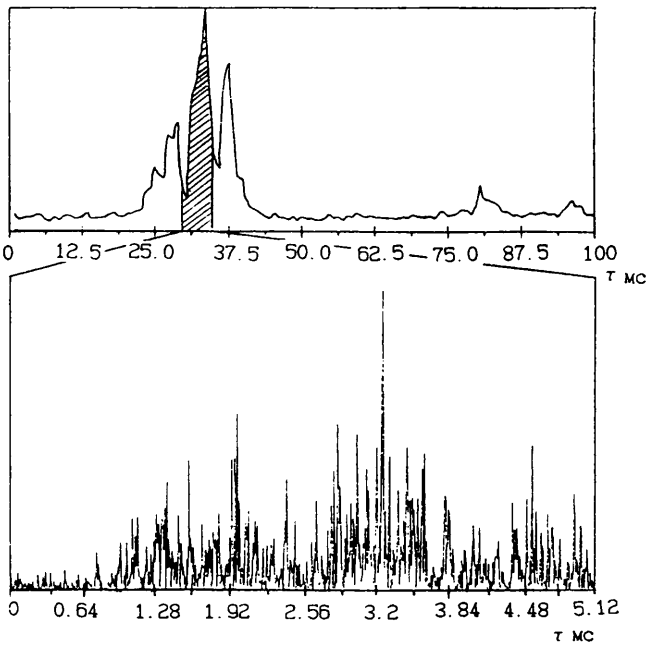

Figure 1 Intensity curve of a single pulse of PSR 0809+74. The curve was smoothed with time consistent of 0.8 ms. In the bottom of the figure the chosen part of subpulse is shown with a resolution of 10 μs.

In figure 1 (top part) the intensity curve of a single pulse from PSR 0809+74 is shown. The curve was smoothed with a time constant of 0.8 ms. In the bottom of the figure the chosen part of the pulse is shown with a resolution of 10 μs. We limit ourselves to a duration of the selected part of the subpulse equal to 5.12 ms ($N = 512$). Some examples of data processing are shown in figure 2.

A log-log plot of the correlation integral $C(r)$ versus distance r is presented on the left side of the figure. This part shows the linear range of the slope according to eq.(6). With increasing dimension d of the constructed phase space, the slope converges towards a limiting value. This slope behavior is shown as a function of the dimension d of the constructed phase space in the lower right part of figure 2. For the given subpulse $S(t)$-curve ν reaches the limiting value of 5.3 in a twenty-dimensional phase space. Such behavior is typical for a chaotic dynamical system. In the upper right part of figure 2 we show the second-order entropy K_2 as a function of dimension d for the same subpulse. The corresponding limiting value of correlation time is 32 μs for the case.

Using this technique we have processed 480 single pulses from PSR 0809+74 and 206 off-pulse records. The dependence of the slope ν versus the embedding dimension d is shown in figure 3 for the off-pulse record (uncorrelated band-limited white noise of the receiver). One can see that in this case there is no saturation of ν in the twenty dimensional phase space.

https://doi.org/10.1017/S0002731600155441 Published online by Cambridge University Press

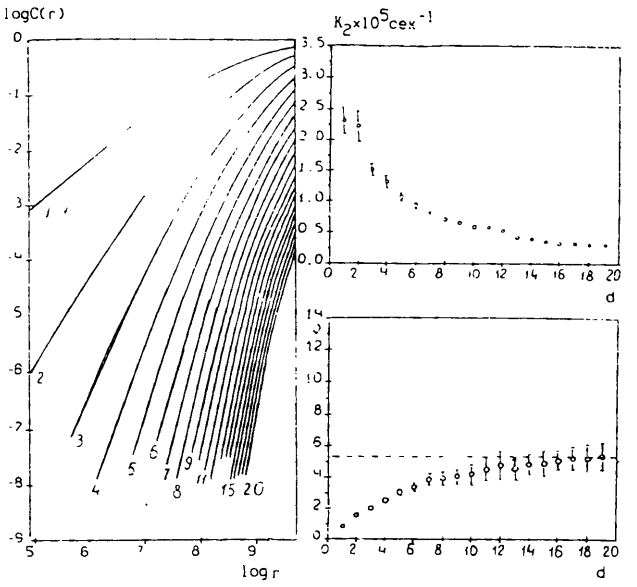

Figure 2 Log-log plot of the correlation integral $C(r)$ *vs.* the distance r (left side). The behavior of the slope of the linear part of $C(r)$ is shown as a function of the dimension d of the constructed phase space in the lower right part of the figure. The upper right part of the figure shows a second-order entropy K_2 as a function of dimension d.

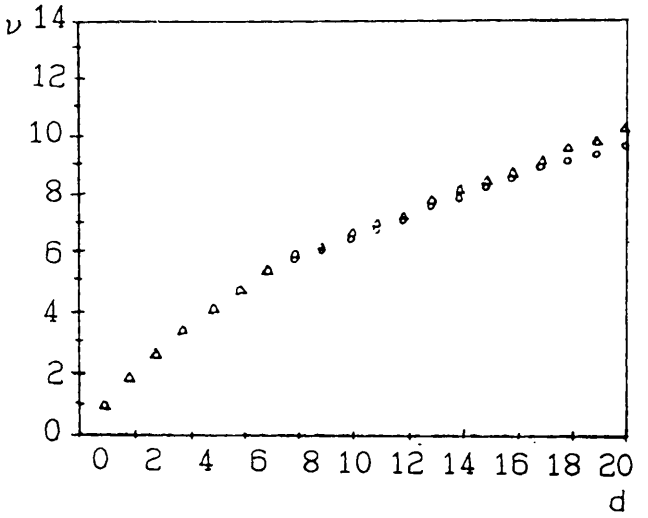

Figure 3 The dependence of the slope ν *vs.* the embedding dimension d for the off-pulse record (uncorrelated band-limited white receiver noise).

Results

The results of our analysis are shown in figure 4 (a,b,c,d). For each processed subpulse we have determined the saturated value of ν, which we call the correlation dimension ν_c. To get the value of ν_c we approximated the $\nu \propto (d)$ curve using a parabolic function and took the maximum ordinate of the parabola to be ν_c. The same technique has been applied to the off-pulse records. A comparison of the ν_c distributions obtained for the pulse and off-pulse

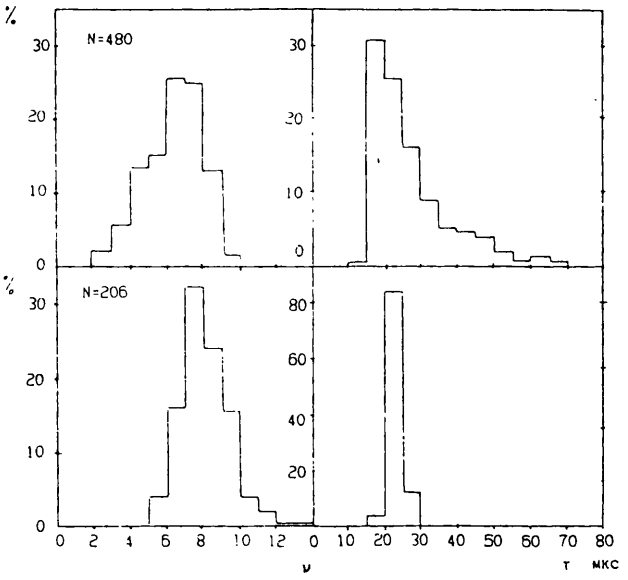

Figure 4 The comparison of the distributions of ν_c and τ_c for pulse and off-pulse emission.

emission is presented in figure 4a and b. We can see that in off-pulse records there are no occasions with $\nu_c \leq 5$, while in on-pulse analysis such low-dimensional realizations contribute more than 20% to the distribution. An even more drastic difference is between distributions of the correlation time for on-pulse and off-pulse records (figure 4c and d). For the off-pulse data the distribution occupies nearly the only bin of 20–25 μs. For the on-pulse data the correlation-time (τ_c) distribution starts at 60–70 μs and rapidly increases with decreasing τ_c up to the limit of our time resolution. We would like to note that the maximum of this distribution occurs in the 15–20 μs bin—that is, shorter than for the receiver noise.

Conclusions

1. The microstructure modulation of pulsar radio emission may be described by the model of low-dimensional deterministic chaos in 20% of occasions. On such occasions the temporal structure of the micropulse emission may be interpreted as a reflection of the spatial structure of the relevant plasma outflow, which is in the early stage of turbulence.

2. The distribution of the correlation time shows a steady increase to the shortest observable time bin, and demonstrates a tendency for microstructure to consist of a random sequence of unresolved micropulses in the majority of cases.

https://doi.org/10.1017/S0002731600155441 Published online by Cambridge University Press